*32nd EPS Conference on Plasma Phys. Tarragona, 27 June - 1 July 2005 ECA Vol.**29C**, P-4.084 (2005)*

Fast Electron Bremsstrahlung in Arbitrary Tokamak Configuration

Y.Peysson, J. Decker[+], F. Imbeaux and D. Mazon

Association Euratom-CEA, CEA/DSM/DRFC, CEA-Cadarache, 13108, Saint Paul lez Durance, France
[+] Plasma Science and Fusion Center, MIT, Cambridge, MA-02139, USA

1. Introduction

During the last past years, the non-thermal plasma bremsstrahlung emission has proven to be a very powerful tool for investigating the build-up of a non-thermal electron tail in the range of energy 20-200 keV by resonant interaction between plasma and radio-frequency (RF) waves [1]. Following the pioneering work done on the tokamak Tore Supra [2], tomographic systems with a large number of chords and refined spectrometric capabilities have therefore been installed on numerous toroidal devices. Most of them are dedicated to detailed observations of the hard x-ray (HXR) emission profile at different photon energies in a poloidal cross-section of the plasma, [3-5], while few are concerned by angular dependence studies along the toroidal direction, and relativistic effect which is the signature of very energetic electrons [6].

Despite numerous attempts, it has never been possible to invert the line-integrated HXR profile, and extract directly from measurements the shape of the electron momentum distribution function at different plasma locations. Since this problem is deeply ill-conditioned, HXR Abel inverted studies are only used to qualitative analysis, assuming that bremsstrahlung emission is a flux surface quantity, an assumption which is sometimes questionable when RF power absorption is well off-axis. Indeed, experimental observations have clearly shown lack of symmetry between high and low magnetic field side regions [1,2], a difference which may results not only from Shafranov shift, but also from the presence of trapped electrons, and also the complex combination between forward emission and helical field lines.

A quantitative assessment of the consistency between line-integrated non-thermal bremsstrahlung emission and plasma current in fully non-inductive regimes requires therefore a complete description of the physical process at play, including the complexity that results from the interplay between momentum and radial spaces dynamics. Calculations here presented are performed using relativistic electron distribution functions deduced from a fast 3-D bounce-averaged electron drift-kinetic solver dedicated to the current drive problem in arbitrary plasma configuration [7]. Comparison with experimental observations is presented.

2. Bremsstrahlung calculations

The number of counts N_{E0} that is recorded in the energy range $E_0 \pm \Delta E$ between times t_{min} and t_{max} is given by the integral

$$N_{E_0} = \int_{t_{\min}}^{t_{\max}} dt \int_{E_0-\Delta E}^{E_0+\Delta E} \frac{dN_E\,(t,E)}{dtdE} dE$$

where $dN_E(t)/dt\Delta E$ is the measured photon energy spectrum. It is related to the effective photon energy spectrum $dN_k(t)/dtdk$ emitted by the plasma in the direction of the detector by

$$\frac{dN_E\,(t,E)}{dtdE} = \int_0^{\infty} \eta_A\,(k)\,(1-\eta_D\,(k))\,G\,(k,E)\,\frac{dN_k\,(t,k)}{dtdk} dk$$

where $G(k,E)$ is the normalized instrumental response function, $\eta_A(k)$ is the fraction of photon transmitted rather than being absorbed by various objects along the line-of-sight, and $1-\eta_D(k)$ is the fraction stopped inside the active part of the photon detector.

Since the plasma is an extended source of photons, all contributions inside the volume ΔV viewing the detector with a solid angle ΔΩ must be added, taking into account that photon plasma

$$\frac{dN_k\left(t,k\right)}{dtdk}=\int_{\Delta V(k)}dV\int_{\Delta\Omega(k)}\frac{dN_k\left(t,k,\mathbf{X},\widehat{b}\cdot\widehat{d}\right)}{dtdkdV\,d\Omega}d\Omega$$

emission depends not only of the plasma position **X** (inhomogeneity), but also of the angle $\hat{b}\cdot\hat{d}$ between the directions of the magnetic field line and the line-of-sight.

In the limit of a small diaphragm aperture, variation of the emission transverse to the chord may be neglected, and

where $n_k = dN_k/dV$ is the photon density, l_{max}-l_{min} is the chord length inside the plasma and $\mathcal{G}_{\mathcal{D}}$ is a fixed geometrical factor for each line-of-sight. Assuming that the magnetic field line is locally an axis of symmetry for the electron velocity distribution function and that the velocity direction for each electron is also an axis of symmetry for the probability of photon emission, one obtains,

$$\frac{dn_k\left(t,k,\mathbf{X},\widehat{b}\cdot\widehat{d}\right)}{dtdkd\Omega}=\sum_{m=0}^{\infty}\left(m+1/2\right)I_B^{(m)}\left(t,\mathbf{X},p,k\right)P_m\left(\widehat{b}\cdot\widehat{d}\right)$$

where P_m is the Legendre polynomial of order m, and the bremsstrahlung function $I_B^{(m)}$ is

$$I_B^{(m)}\left(t,\mathbf{X},p,k\right)=2\pi\int_0^{\infty}vp^2f^{(m)}\left(t,\mathbf{X},p\right)\left[\sum_s n_s\left(t,\mathbf{X}\right)\frac{d\sigma_{ei}^{(m)}\left(k,p,Z_s\right)}{dtdkd\Omega}\,dp+n_e\left(t,\mathbf{X}\right)\frac{d\sigma_{ee}^{(m)}\left(k,p\right)}{dtdkd\Omega}\right]dp$$

where v and p are respectively the electron velocity and momentum, $f^{(m)}$ is the projection of the electron distribution on the Legendre polynomial basis, n_e is the electron density, n_s is the density of species s, σ_{ei} and σ_{ee} the electron-ion and electron-electron relativistic bremsstrahlung cross-sections. By definition n_e and n_s are flux-surface functions and depends only of ψ, the poloidal flux coordinate, while

$$\frac{d\sigma_{ei}^{(m)}\left(k,p,Z_s\right)}{dtdkd\Omega}=\int_{-1}^{+1}\frac{d\sigma_{ei}^{(m)}\left(k,p,\widehat{k}\cdot\widehat{p},Z_s\right)}{dtdkd\Omega}P_m\left(\widehat{k}\cdot\widehat{p}\right)d\left(\cos\chi\right)$$

and

$$f^{(m')}\left(t,\mathbf{X},p\right)=\int_{-1}^{+1}f\left(t,\mathbf{X},p,\xi\right)P_{m'}\left(\xi\right)d\xi$$

Here, $f\left(t,\mathbf{X},\mathbf{p}\right)=f_0\left(t,\theta,\psi,p,\xi\right)$ is the electron distribution function at poloidal position θ, deduced from $f_0^{(0)}\left(t,\psi,p,\xi_0\right)$ at $B = B_{min}$, solution of the zero-order bounce-averaged 3-D relativistic Fokker-Planck [**]. The pitch-angles ξ and ξ_0 are linked by the simple relation $\xi=\sigma\sqrt{1-\Psi\left(\psi,\theta\right)\left(1-\xi_0^2\right)}$ where $\Psi\left(\psi,\theta\right)=B\left(\psi,\theta\right)/B_{\min}\left(\psi\right)$ and $\sigma=\xi/|\xi|$. With this formalism, it is possible to consider first order corrections of the electron distribution function, which result from vertical drift corrections. However, except in very localized region of the plasma where pressure gradient is large, like in internal transport barrier, this correction is almost negligible.

Numerical calculations are carried out in four steps. From the knowledge of $f_0^{(0)}\left(t,\psi,p,\xi_0\right)$, $f_0\left(t,\theta,\psi,p,\xi\right)$ is first determined at each poloidal and radial position on a 2-D mesh. In Fig. 1, differences between low and high field sides are displayed.

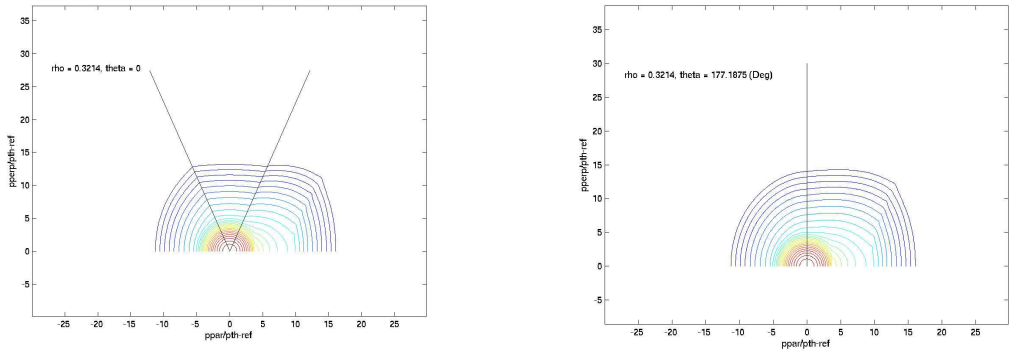

Fig.1. Contours of the electron momentum distribution function for a Lower Hybrid current drive discharge on the low magnetic field side (left) and high magnetic field side (right), at the same radial position $\rho = 0.32$. In the high magnetic field region, only circulating electrons are concerned.

Then, chord length Δl and $\hat{b}\cdot\hat{d}$ for each elementary plasma volume $\Delta V = \dfrac{2\pi r R}{\hat{\psi}\cdot\hat{r}}\dfrac{\Delta\psi\Delta\theta}{|\nabla\psi|}$ are calculated, taking into account of the safety factor profile $q(\psi)$, the directions of the magnetic field and the plasma current according to the magnetic equilibrium that is studied. In Fig. 2, the (ψ,θ) grid is shown as well as the lines-of-sight of the tomographic system installed on Tore Supra in the configuration corresponding to the experimental campaign of 1999 [2].

Projections of the bremsstrahlung cross-sections and the distribution function at (ψ,θ) positions on the Legendre polynomial basis are determined by a Gaussian quadrature which ensures a high numerical accuracy even for large *m* values corresponding to strongly oscillating polynomials. For most situations encountered in current drive experiments, calculations are performed with *m = 50*. An example of the quality of the reconstruction of the electron distribution function is given in Fig. 3 for a simulation of Lower Hybrid current drive experiments, considering a normalized quasilinear diffusion coefficient $D_{LH} \approx 0.5$ in the interval $3.5 \le v_P/v_{th} \le 7$.

3. Comparison with experiment

Calculations here presented are performed for a typical Lower Hybrid full current drive discharge, where power absorption is rather off-axis (peaked at ρ≈0.3). In the range of photon energy 60-80 keV, the line-integrated HXR profile given by the vertical camera shown in Fig. 2 is clearly non-symmetric regarding to the high-low magnetic field side regions (Fig. 4). This effect, which is well beyond experimental uncertainty is systematic in these regimes. This kind of discharge has been simulated using the numerical magnetic equilibrium solver HELENA [**], describing the absorption of the Lower Hybrid wave by a Gaussian radial dependence of the form $D_{LH} = D_{LH}^0 \exp\left(-(\rho-\rho_{LH})^2/\Delta\rho_{LH}^2\right)$, with $\rho_{LH} = 0.3$ and $\Delta\rho_{LH} = 0.2$, the absorbed power spectrum being independent of the radial position. As shown in Fig. 5, the lack of symmetry is well reproduced by the model, with the correct relative amplitude. A detailed analysis has shown that both the variation of the safety factor and the Shafranov shift have negligible contributions, and this effect is only the consequence of the presence of trapped electrons in the low field side region. This result demonstrates for the first time the role played by bouncing electrons which reduce the non-thermal bremsstrahlung level, because their perpendicular energy is larger as compared to circulating one. The very good agreement confirms that the electron distribution function in non-inductive regime is dominated by collisional slowing-down including neoclassical effects and support a weak anomalous radial transport.

Simulations have been also performed for RFP magnetic configuration, confirming in that case the large role played by the q-factor of the HXR intensity in PPCD regimes, conversely to the usual tokamak configuration [4].

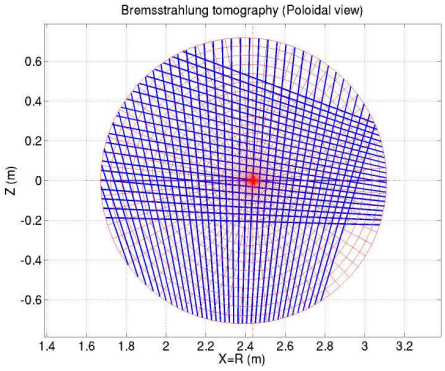

Fig.2: HXR tomographic configuration for Tore Supra tokamak (1999 experimental campaign), and plasma magnetic equilibrium.

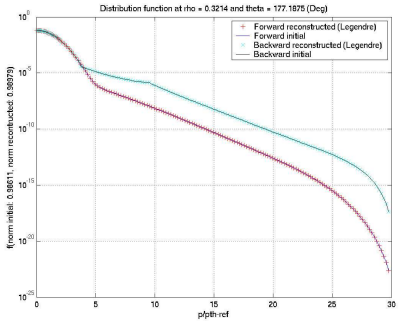

Fig.3. Comparison between initial and reconstructed distribution function (backward and forward directions) after Legendre polynomial projection at ρ=0.32.

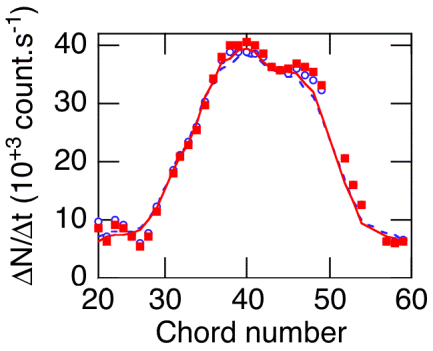

Fig. 4. Experimental observation of the HXR emission during a full LHCD discharge (vertical camera, see, Fig. 2), in the range of photon energy 60-80 keV

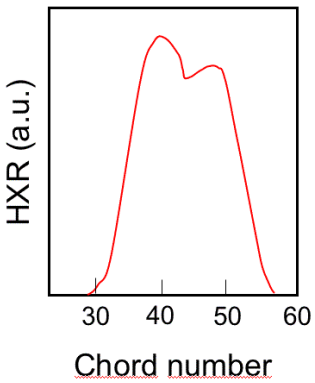

Fig. 5. Simulation of the HXR emission profile for the LHCD discharge shown in Fig. 4. The lack of HFS-LFS symmetry is mainly due to trapped electrons

[1] «Towards Steady-State Sustainment of Electron Transport Barrier in TORE SUPRA», by Y. Peysson et al., in Advances in Plasma Physics Research, (2003) Vol. 4, Nova Science Publishers (New York, USA) p. 1.
[2] Y. Peysson and F. Imbeaux, **70** (1999) 3987.
[3] S. Coda et al., Nucl. Fusion **43** (2003) 1361.
[4] R. O'Connell et al. Phys. Rev. Lett. **91** (2003) 045002.
[5] J. Liptac, for the tokamak C-MOD, Private communication.
[6] Z.Y. Chen et al. Nucl. Instr. and Methods in Phys. Research **A 543** (2005) 602.
[7] J. Decker and Y. Peysson, Euratom-CEA report EUR-CEA-FC-1736 (2004).